


# Phylogenetic and Phylogeographic Analysis of the Highly Pathogenic H5N6 Avian Influenza Virus in China

Hanlin Liu <sup>1,2,3,†</sup> , Changrong Wu <sup>1,2,3,†</sup>, Zifeng Pang <sup>1,2,3</sup>, Rui Zhao <sup>1,2,3</sup>, Ming Liao <sup>4,5,\*</sup> and Hailiang Sun <sup>1,2,3,\*</sup>

<sup>1</sup> College of Veterinary Medicine, South China Agricultural University, Guangzhou 510642, China

<sup>2</sup> Key Laboratory of Zoonosis Control and Prevention of Guangdong Province, South China Agricultural University, Guangzhou 510642, China

<sup>3</sup> National and Regional Joint Engineering Laboratory for Medicament of Zoonosis Prevention and Control, South China Agricultural University, Guangzhou 510642, China

<sup>4</sup> Institute of Animal Health, Guangdong Academy of Agricultural Sciences, Guangzhou 510640, China

<sup>5</sup> Key Laboratory for Prevention and Control of Avian Influenza and Other Major Poultry Diseases, Ministry of Agriculture and Rural Affairs, Guangzhou 510640, China

\* Correspondence: mliao@scau.edu.cn (M.L.); hsun@scau.edu.cn (H.S.)

† These authors contributed equally to this work.

**Abstract:** The clade 2.3.4.4b H5N8 avian influenza viruses (AIVs) have caused the loss of more than 33 million domestic poultry worldwide since January 2020. Novel H5N6 reassortants with hemagglutinin (HA) from clade 2.3.4.4b H5N8 AIVs are responsible for multiple human infections in China. Therefore, we conducted an epidemiological survey on waterfowl farms in Sichuan and Guangxi provinces and performed a comprehensive spatiotemporal analysis of H5N6 AIVs in China. At the nucleotide level, the H5N6 AIVs isolated in the present study exhibited high homology with the H5N6 AIVs that caused human infections. Demographic history indicates that clade 2.3.4.4b seemingly replaced clade 2.3.4.4h to become China's predominant H5N6 AIV clade. Based on genomic diversity, we classified clade 2.3.4.4b H5N6 AIV into ten genotypes (2.3.4.4bG1–G10), of which the 2.3.4.4bG5 and G10 AIVs can cause human infections. Phylogeographic results suggest that Hong Kong and Jiangxi acted as important epicentres for clades 2.3.4.4b and 2.3.4.4h, respectively. Taken together, our study provides critical insight into the evolution and spread of H5N6 AIVs in China, which indicates that the novel 2.3.4.4b reassortants pose challenges for public health and poultry.

**Keywords:** H5N6 avian influenza virus; 2.3.4.4b reassortant; evolution; phylogeographic analysis



**Citation:** Liu, H.; Wu, C.; Pang, Z.; Zhao, R.; Liao, M.; Sun, H.

Phylogenetic and Phylogeographic Analysis of the Highly Pathogenic H5N6 Avian Influenza Virus in China. *Viruses* **2022**, *14*, 1752. <https://doi.org/10.3390/v14081752>

Academic Editors: Samantha Lycett and Paul Digard

Received: 23 July 2022

Accepted: 9 August 2022

Published: 11 August 2022

**Publisher's Note:** MDPI stays neutral with regard to jurisdictional claims in published maps and institutional affiliations.



**Copyright:** © 2022 by the authors. Licensee MDPI, Basel, Switzerland. This article is an open access article distributed under the terms and conditions of the Creative Commons Attribution (CC BY) license (<https://creativecommons.org/licenses/by/4.0/>).

## 1. Introduction

The genetics and antigens of H5 AIVs, which circulate in wild birds and poultry globally, are diverse [1]. To date, H5 AIVs have evolved into different phylogenetic clades (clade 0–9) [2], and clade 2.3.4.4 has further evolved into eight subclades (2.3.4.4a–2.3.4.4h) according to the World Health Organization's naming system [3]. H5 AIVs with the HA of clade 2.3.4.4b have been detected in wild birds and poultry worldwide [4–6] and have caused the loss of more than 33 million domestic poultry across the globe (<https://empres-i.apps.fao.org/>; accessed on 28 April 2022). Novel H5N6 reassortants were reported as one of the dominant AIV subtypes in China, especially in ducks, during 2014–2016 [7]. The clade 2.3.4.4h viruses became the dominant H5N6 lineage in China during 2018–2020 through continually evolving [8,9]. H5N8 AIVs with the HA of clade 2.3.4.4b are responsible for a new wave of outbreaks in poultry and wild birds in January 2020 [10,11]. Currently, the novel H5N6 reassortants with the HA from clade 2.3.4.4b H5N8 AIVs emerged in waterfowl and have caused human infections in China [12,13]. In this study, we conducted an epidemiological survey on local waterfowl farms in Sichuan and Guangxi provinces and performed a comprehensive spatiotemporal analysis of H5N6 AIVs in China from 2017 to May 2022. Our findings provide novel insight into the latest spatiotemporal characteristics of H5N6 AIVs and highlight their potential threat to public health.

## 2. Materials and Methods

### 2.1. Virus and Sequence Preparation

Two H5N6 AIVs designated as A/duck/Sichuan/SS1/2021 and A/goose/Guangxi/GG1/2022 were isolated from lung samples of waterfowl farms in Sichuan and Guangxi. The whole genome was amplified using universal primers [14]. All viral experiments were conducted in Biosafety Level 3 (BSL-3) facilities. All available H5N6 sequences isolated in China from 2017 to May 2022 were retrieved from the Global Initiative on Sharing All Influenza Data databases (GISAID; <https://www.gisaid.org>; accessed on 15 May 2022). Sequences with (a) evidence of lab errors and (b) 100% similarity were discarded. Detailed information on all H5N6 AIVs analysed in this study can be found in Table S1.

### 2.2. Maximum Likelihood Phylogenetic of the H5N6 AIVs

Sequence alignments were constructed for eight segments separately using the MAFFT (version 7.149) program [15]. Using ModelFinder, the best-fit model was GTR+F+G4 [16]. Phylogenetic trees were inferred using the maximum likelihood method in the IQ-TREE 1.68 software with 1000 bootstraps [17,18]. We used ITOL (version 5) to complete the annotation of the evolutionary tree and to adjust it aesthetically [19]. The genotypes of the H5N6 AIVs were classified according to the combinations of lineages in segment trees (Figures S3–S10) [7,12,18].

### 2.3. Bayesian Maximum Clade Credibility Phylogenetic and Demographic Analysis of the H5N6 AIVs

We used the TempEst (version 1.5.3) software to assess the temporal signals by performing root-to-tip regression analysis on viruses from clades 2.3.4.4b and 2.3.4.4h [20], which showed strong temporal signals suitable for demographic history analysis (Figure 1a,b). We computed marginal likelihoods using path sampling and stepping-stone sampling to compare the constant-size, exponential-growth and Bayesian skyline coalescent tree priors [21], and to compare the strict molecular clock and uncorrelated lognormal relaxed clock [22]. The best-fit model was chosen to construct Bayesian maximum cluster credibility (MCC) trees, utilising 300,000,000 total steps for each set, sampling every 1000 steps (Tables S2 and S3). The convergence (effective sample sizes > 200) of relevant parameters was assessed using Tracer (version 1.7) [23]. TreeAnnotator (version 1.10.4) software was used to summarize the information from a sample of trees produced by BEAST on a single “target” tree to obtain the MCC tree. The phylogenetic tree was visualised in FigTree version 1.4.3 (<http://tree.bio.ed.ac.uk/software/figtree/>; accessed on 15 June 2022).

### 2.4. Phylogeographic Interference

We used the Bayesian stochastic search variable selection (BSSVS) model with asymmetric substitution to infer the H5N6 AIV spread dynamics from 2017 to May 2022 in China [24]. In order to reduce the sampling biases, we used CD-HIT v4.6 to remove viruses without known regional information and identical sequences [25], and further subsampled the dataset in a stratified manner to create the balanced number of sequences per region, which resulted in the final dataset including 28 viruses of clade 2.3.4.4b and 111 viruses of clade 2.3.4.4h (Figures S1 and S2). We considered transitions credible when the Bayes factor (BF) was >3 and used spread3 v0.9.6 to compute the BF tests to assess the support for significant individual transitions between distinct geographic regions [24,26]. We provide detailed information on BF values, migration rates and distances of clades 2.3.4.4b and 2.3.4.4h H5N6 AIVs in Table S4.

## 3. Results and Discussion

Molecular analysis revealed that all H5N6 AIVs in this study possess the same polybasic amino acid motif of -RRKR/GLF- in their HA cleavage site, which is a highly pathogenic avian influenza virus (HPAIV) characteristic (Table S2). It is noteworthy that all H5N6 AIVs contained more than one of the seven HA amino acid mutations (94N, 133A, 154D, 155N,

156A, 188I and 189R), which could increase virus binding to  $\alpha 2$ , 6-linked sialic acid receptors [27–31]. Furthermore, most H5N6 AIVs contain the M1 15I, NS1 103F and NS1 106M mutations associated with virulence, transmission, replication efficiency and adaptation in mammals [32–34]. At the nucleotide level, two viruses isolated in our study exhibited high homology with those that cause human infections in the same provinces. The nucleotide homology for the eight genes was 98.88–99.60% between A/duck/Sichuan/SS1/2021 and A/Sichuan/06681/2021 and 95.18–99.61% between A/goose/Guangxi/GG1/2022 and A/GX/guilin/11151/2021 (Table 1).

**Table 1.** Nucleotide sequence identity between the virus isolated in this study with virus isolated in human available in GISAID <sup>a</sup>.

Virus Isolated in This Study with Virus Isolated in Humans	Fragment <sup>b</sup>	Identity (%)
A/duck/Sichuan/SS1/2021 with A/Sichuan/06681/2021	PB2	99.60
	PB1	99.46
	PA	99.39
	HA	99.58
	NP	99.39
	NA	95.49
	M	99.16
	NS	98.88
A/goose/Guangxi/GG1/2022 and A/GX/guilin/11151/2021	PB2	98.84
	PB1	99.33
	PA	99.23
	HA	99.41
	NP	99.39
	NA	95.18
	M	99.49
	NS	99.61

<sup>a</sup> <https://www.gisaid.org>; accessed on 15 May 2022. <sup>b</sup> Polymerase basic subunit (PB); Polymerase acidic subunit (PA); Hemagglutinin (HA); Nucleoprotein (NP); Neuraminidase (NA); Matrix (M); Non-structural (NS).

We found that clades 2.3.4.4c, 2.3.4.4e and 2.3.4.4g contained relatively few viruses (Figure S3). Therefore, we used a virus branch to show the population of clades 2.3.4.4c and 2.3.4.4g and a histogram to represent the population of clade 2.3.4.4h (Figure 1c). Meanwhile, the estimated effective population size showed a sharp expansion of clade 2.3.4.4b H5N6 AIVs in 2020–2021, which is consistent with estimations when a new wave of clade 2.3.4.4b H5N8 entered China [35], and a continuous decline of clade 2.3.4.4h H5N6 AIVs in 2019–2022 (Figure 1c). Therefore, clade 2.3.4.4b seemingly replaced clade 2.3.4.4h to become the predominant lineage in China. Remarkably, the cross-host barrier transmission events of clade 2.3.4.4b H5N6 AIV expanded its host range to at least six species, including humans (Figure 1c).

Additional phylogenetic analyses of the internal genes of H5N6 AIVs revealed that the PB2, PB1, PA, NP, M and NS genes classified into five (Figure S5), five (Figure S6), six (Figure S7), four (Figure S8), five (Figure S9) and five (Figure S10) separate lineages, respectively. The internal genes of clade 2.3.4.4h H5N6 AIVs were mainly derived from the H6, H5N6 and H5N1 viruses, while the internal genes of clade 2.3.4.4b AIVs were primarily derived from the H5N8, H3N2, H5N1 and H7N9 viruses (Figure 2). Moreover, except for A/duck/China/0938/2017, almost all 2.3.4.4b H5N6 AIVs bore internal genes from the H5N8 virus (Figure 2). Therefore, the increasing genetic reassortment between H5N6 and H5N8 AIVs may pose an even greater threat to the poultry industry and public health.

To further reveal H5N6's evolutionary characteristics, we conducted molecular clock phylogenetic analysis and genotype characterisation (Figure 2). Based on genomic diversity, clade 2.3.4.4b H5N6 AIVs were classified into ten different genotypes (2.3.4.4bG1–G10) (Figure 2), of which the 2.3.4.4bG5 and G10 AIVs caused human infections [12,13]. More specifically, 2.3.4.4bG5 viruses bore the NA gene from the Eurasian lineage, the PB2, PB1,

PA and the NS genes from the H3N2 virus, the NP gene from the H5N1 virus and the M gene from the H5N8 virus. The 2.3.4.4bG10 viruses contain the NA gene from the Eurasian lineage, the PB2 and PB1 genes from the H3N2 virus, the NP and NS genes from the H5N1 virus and the M gene from the H5N8 virus (Figure 2; Table S2). The genotypes of clade 2.3.4.4b H5N6 AIVs were most diverse in waterfowl, which are considered an essential reservoir for AIVs [36,37]. Moreover, 2.3.4.4b H5N6 AIVs exhibited distinct antigenicity to the Re-11 vaccine strain, which increases the risk to poultry [13].

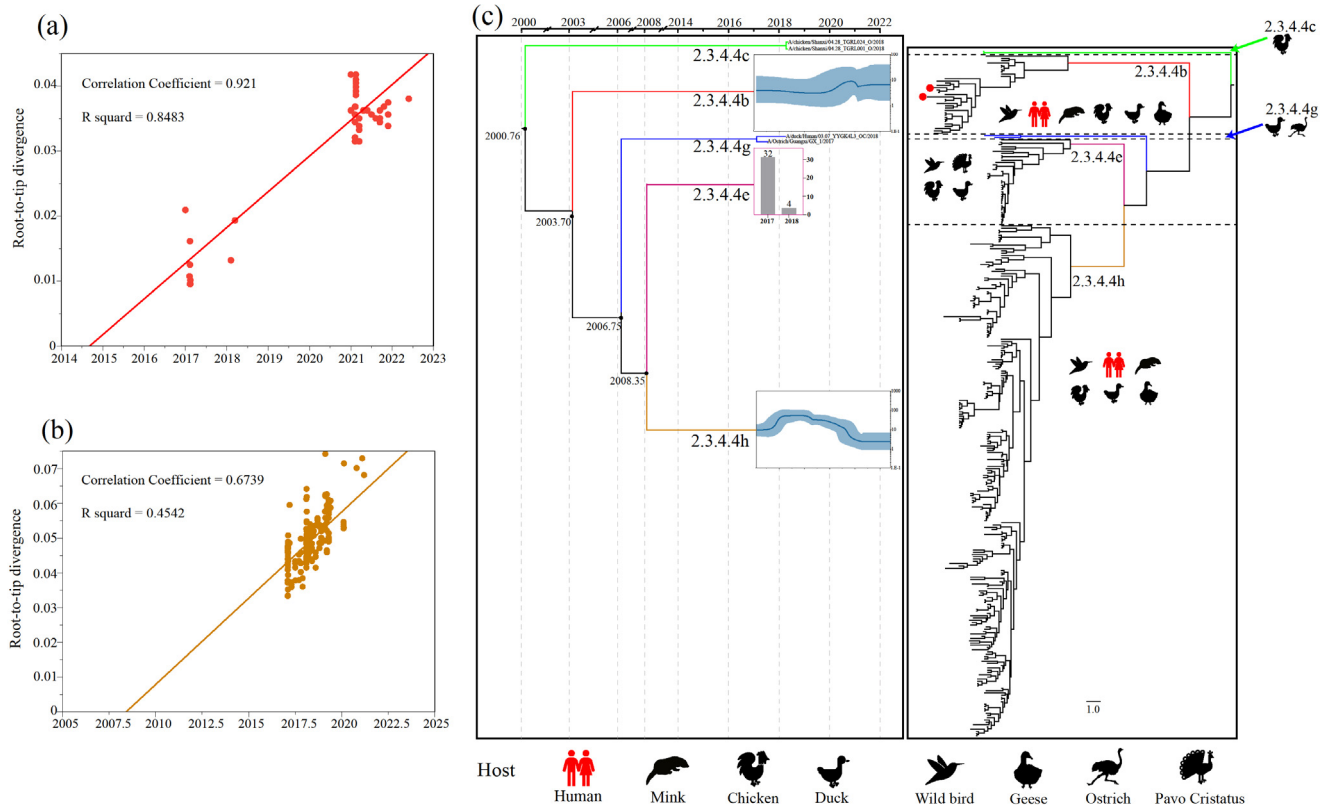


**Figure 1.** Population evolutionary relationships of the H5N6 AIVs in China during 2017–May 2022. (a) The temporal signal of clade 2.3.4.4b H5N6 AIVs root-to-tip regression analysis. (b) The temporal signal of clade 2.3.4.4h H5N6 AIVs root-to-tip regression analysis. (c) Classification and evolutionary history of H5N6 AIVs. (Left) Summary of coalescence analyses of the overall H5N6 sequences in China during 2017–May 2022, performed in BEAST (1.10.4). The blue curve inside the box is a Bayesian skyline plot (BSP), and the light blue curves represent upper and lower 95% highest probability density (HPD) values. The y axis of each BSP is relative genetic diversity, represented on a log<sub>10</sub> scale. For some of the lineages (Clade 2.3.4.4c, 2.3.4.4e, and 2.3.4.4g), BSP was not performed because of the limited sample size. In the 2.3.4.4c and 2.3.4.4g lineages, we showed the branch of the viruses. In the 2.3.4.4e lineage, we used histograms instead, and the y-axis of each histogram shows the number of samples. The timeline of each lineage is aligned with the timeline of MCC tree. (Right) Overall phylogeny constructed using BEAST. The host range of each lineage was represented by animal icons.

Using a phylogeographic approach, we then estimated the migration pathways of clade 2.3.4.4b and 2.3.4.4h. There were 22 and 35 statistically significant migrations in clades 2.3.4.4b and 2.3.4.4h, respectively (Table S4). The long-distance migrations of clades 2.3.4.4b and 2.3.4.4h occurred between Xinjiang and other regions (Figure 3a,d). The H5N6 AIVs from 2017 to May 2022 migrations of clades 2.3.4.4b and 2.3.4.4h also occurred between close regions (Figure 3b,e), and the transition rates between regions were inversely related to the distance (Figure 3c,f). These findings indicate that AIV migrations occur more frequently at shorter distances, consistent with a previous study [38]. The inferred spatial dynamics of

H5N6 AIVs suggest that Hong Kong and Jiangxi acted as important epicentres of clades 2.3.4.4b and 2.3.4.4h H5N6 AIVs, respectively (Figure 3a,b). A previous study supports that the live poultry trade between different regions may facilitate the geographic migration of AIVs [7]. Currently, clade 2.3.4.4b H5N6 AIV is spreading in southern China (Figure 3a,b) and may further spread to other regions, which poses a challenge to public health. There were several limitations in this study. First, sampling bias may affect inference of the spread networks and association between the migration rate and distance. Second, the spatiotemporal HA datasets may not have accurately represented the times and locations of H5N6 AIVs originating in wild birds. Therefore, wild birds as long-distance vectors of HPAIV may result in an increased viral spread, a possibility that was not considered in our study [39,40].

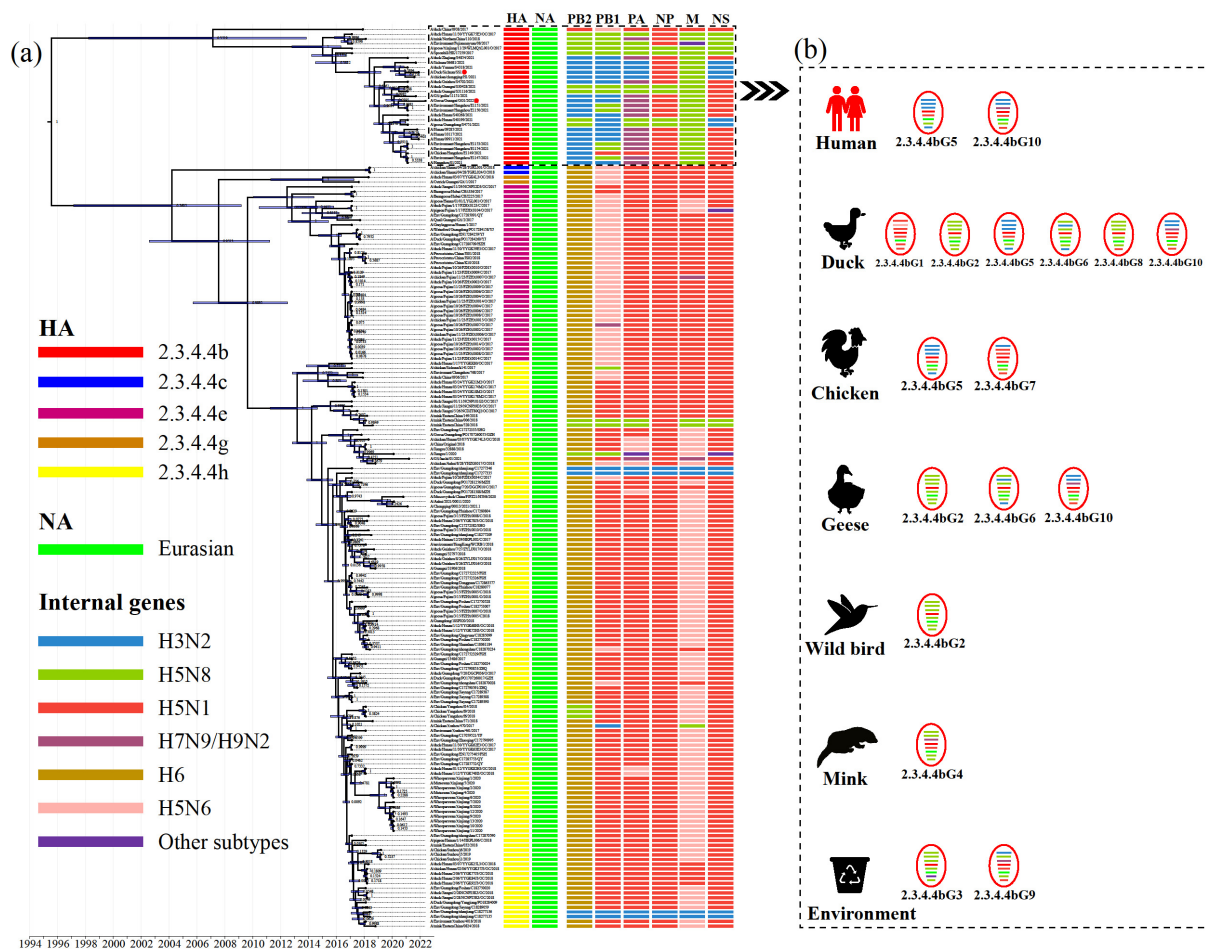


**Figure 2.** Molecular clock phylogenetic analysis of H5N6 AIVs in China during 2017–May 2022. (a) The phylogenetic tree of HA gene using BEAST (version 1.10.4) under the exponential coalescent tree prior model, “GTR+F+G4” substitution mode, and a “uncorrelated relaxed clock” model. The AIVs sequenced in this study were marked with red dots. The lineages of H5N6 AIVs genes were marked by coloured boxes. Purple node bars represented 95% credible intervals of lineage divergence times. (b) The genotype distribution of clade 2.3.4.4b H5N6 AIVs in different hosts. The genotypes of clade 2.3.4.4b H5N6 AIVs isolated in chickens, ducks, geese, minks, wild birds, environments, and humans. The eight segments represented by horizontal bars are, from top to bottom of the virion, PB2, PB1, PA, HA, NP, NA, M, and NS. Different colours represent different lineages. Detailed genotypes are available as the Supplementary Table S2. PB, polymerase basic protein; PA, polymerase acidic protein; HA, hemagglutinin; NP, nucleoprotein; NA, neuraminidase; M, matrix protein; NS, non-structural protein.

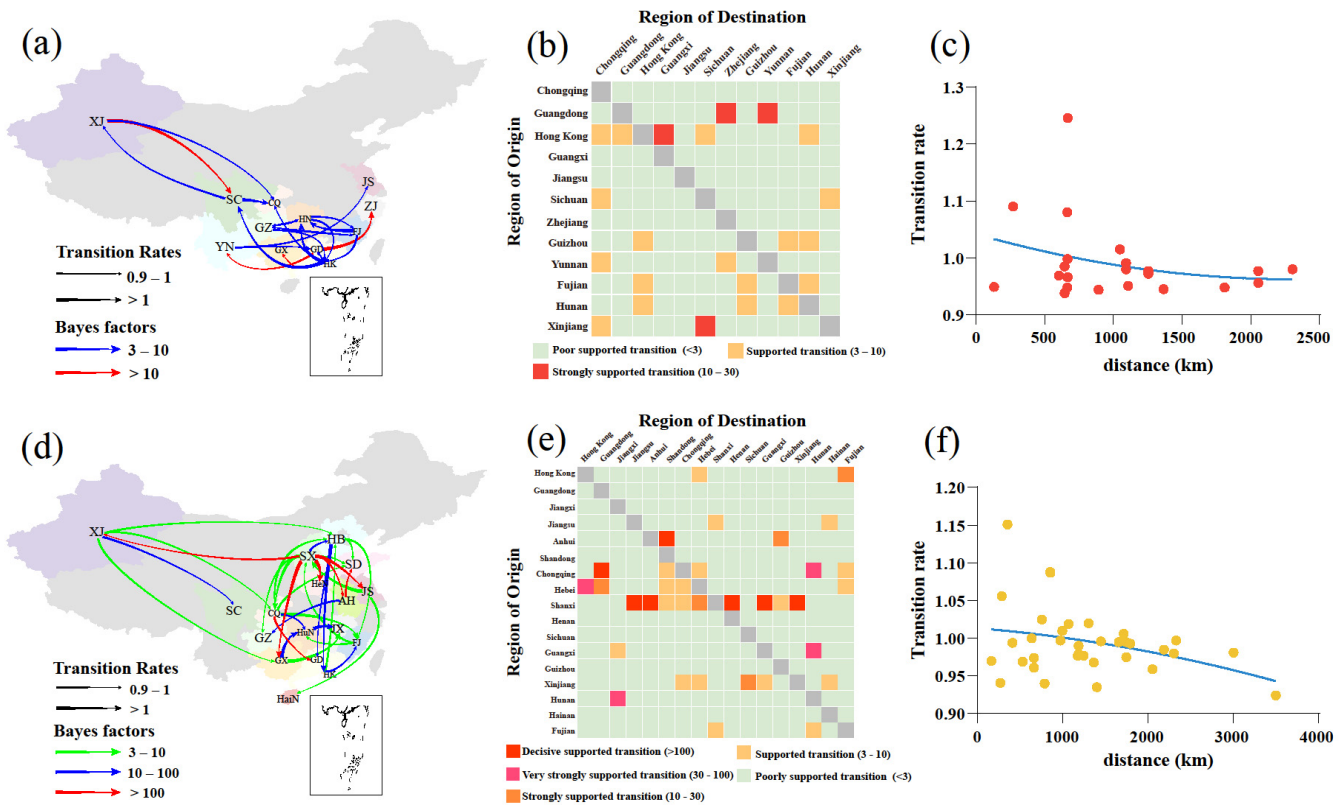


**Figure 3.** Phylogeographic analysis of clade 2.3.4.4b and 2.3.4.4h H5N6 AIVs was determined by Bayesian phylogeographic inference of HA in China during 2017–May 2020. Spatiotemporal spread of clade 2.3.4.4b H5N6 AIVs (a) and clade 2.3.4.4h H5N6 AIVs (d) curves show the inter-region virus transitions statistically supported with Bayes factor (BF) > 3; curve widths represent transition rate values; curve colours represent corresponding statistical BF for each transition rate. The heatmaps display the level of BF for each of the transition pathways considered for clade 2.3.4.4b H5N6 analyses (b) and 2.3.4.4h H5N6 analyses (e), respectively. Inter-region virus transition rates (BF > 3) decrease with geodesic distance between different regions for clade 2.3.4.4b H5N6 AIVs (c) and clade 2.3.4.4h H5N6 AIVs (f), respectively. Abbreviations for the provinces are as follows: HeB: Hebei, CQ: Chongqing, HeN: Henan, SD: Shandong, JS: Jiangsu, HaiN: Hainan, ZJ: Zhejiang, GZ: Guizhou, HuN: Hunan, JX: Jiangxi, AH: Anhui, FJ: Fujian, GD: Guangdong, GX: Guangxi, SC: Sichuan, YN: Yunnan, HK: Hong Kong, XJ: Xinjiang, SX: Shanxi. The map in the square under Guangdong province indicates islands in the South China Sea.

In summary, this spatiotemporal analysis revealed that clade 2.3.4.4b has seemingly become the predominant H5N6 AIV in China. These viruses are genetically diverse among waterfowl and frequently spread in southern China. Moreover, the novel 2.3.4.4bG5 and 2.3.4.4hG10 reassortants can cause human infection, thus, posing a serious threat to public health. Hence, systematic surveillance of the H5N6 AIVs is critical for early warning and preparation for the next potential pandemic.

**Supplementary Materials:** The following supporting information can be downloaded at: <https://www.mdpi.com/article/10.3390/v14081752/s1>, Figure S1: Time-tree of the evolutionary and timescale of clade 2.3.4.4b virus in China. Figure S2: Time-tree of the evolutionary and timescale of clade 2.3.4.4h virus in China. Figures S3–S10: Phylogenetic relationships of all available sequences H5N6 AIVs in China during 2017–May 2022. (S3–S4) The maximum likelihood (ML) phylogenetic trees of the HA and NA genes. (S5–S10) The ML trees of PB2, PB1, PA, NP, M, and NS genes. Table S1: All H5N6 avian influenza viruses in China during 2017–May 2022. Table S2: Detailed information for the full genome of H5N6 viruses analysed in this study. Table S3: Marginal likelihoods of different

combinations of clock model and tree prior. Table S4: Statistically supported migration rates of the clade 2.3.4.4b and 2.3.4.4h H5N6 AIVs.

**Author Contributions:** Conceptualization, H.L., H.S. and M.L.; sample collection, H.S. and C.W.; methodology, H.L., Z.P. and R.Z.; software, H.L. and Z.P.; writing—original draft preparation, H.L. and H.S.; writing—review and editing, H.L., R.Z. and H.S.; supervision, M.L. and H.S. All authors have read and agreed to the published version of the manuscript.

**Funding:** This work was supported by the special fund for scientific innovation strategy-construction of high-level Academy of Agriculture Science-Distinguished Scholar (R2020PY-JC001).

**Data Availability Statement:** Consensus sequences generated in this study were submitted to the GISAID database, and their corresponding accession numbers are listed in Supplementary Table S2.

**Acknowledgments:** We gratefully acknowledge the authors, originating and submitting laboratories of the sequences from GISAID's EpiFlu Database on which this research is based. Colleagues at the College of Veterinary Medicine, South China Agricultural University are thanked for their help in sequencing the isolates.

**Conflicts of Interest:** There are no potential conflict of interest.

## References

- Herfst, S.; Mok, C.K.P.; van den Brand, J.M.A.; van der Vliet, S.; Rosu, M.E.; Spronken, M.I.; Yang, Z.; de Meulder, D.; Lexmond, P. Human Clade 2.3.4.4 A/H5N6 Influenza Virus Lacks Mammalian Adaptation Markers and Does Not Transmit via the Airborne Route between Ferrets. *mSphere* **2018**, *3*, e00405-17. [[CrossRef](#)] [[PubMed](#)]
- WHO; OIE; FAO H5N1 Evolution Working Group. Toward a unified nomenclature system for highly pathogenic avian influenza virus (H5N1). *Emerg Infect. Dis.* **2008**, *14*, e1. [[CrossRef](#)] [[PubMed](#)]
- World Health Organization = Organisation mondiale de la Santé. Antigenic and genetic characteristics of zoonotic influenza A viruses and development of candidate vaccine viruses for pandemic preparedness—Caractéristiques antigéniques et génétiques des virus grippaux A zoonotiques et mise au point de virus vaccinaux candidats pour se préparer à une pandémie. *Wkly. Epidemiol. Rec. = Relev. Épidémiologique Hebd.* **2020**, *95*, 525–539.
- Abolnik, C.; Pieterse, R.; Peyrot, B.M.; Choma, P.; Phiri, T.P.; Ebersohn, K.; Heerden, C.J.V.; Vorster, A.A.; Zel, G.V.; Geertsma, P.J.; et al. The Incursion and Spread of Highly Pathogenic Avian Influenza H5N8 Clade 2.3.4.4 Within South Africa. *Avian Dis.* **2019**, *63*, 149–156. [[CrossRef](#)] [[PubMed](#)]
- Cui, Y.; Li, Y.; Li, M.; Zhao, L.; Wang, D.; Tian, J.; Bai, X.; Ci, Y.; Wu, S.; Wang, F.; et al. Evolution and extensive reassortment of H5 influenza viruses isolated from wild birds in China over the past decade. *Emerg. Microbes Infect.* **2020**, *9*, 1793–1803. [[CrossRef](#)] [[PubMed](#)]
- Shriner, S.A.; Root, J.J.; Lutman, M.W.; Kloft, J.M.; VanDalen, K.K.; Sullivan, H.J.; White, T.S.; Milleson, M.P.; Hairston, J.L.; Chandler, S.C.; et al. Surveillance for highly pathogenic H5 avian influenza virus in synanthropic wildlife associated with poultry farms during an acute outbreak. *Sci. Rep.* **2016**, *6*, 36237. [[CrossRef](#)]
- Bi, Y.; Chen, Q.; Wang, Q.; Chen, J.; Jin, T.; Wong, G.; Quan, C.; Liu, J.; Wu, J.; Yin, R.; et al. Genesis, Evolution and Prevalence of H5N6 Avian Influenza Viruses in China. *Cell Host Microbe* **2016**, *20*, 810–821. [[CrossRef](#)]
- Chen, J.; Li, X.; Xu, L.; Xie, S.; Jia, W. Health threats from increased antigenicity changes in H5N6-dominant subtypes, 2020 China. *J. Infect.* **2021**, *83*, e9–e11. [[CrossRef](#)]
- Li, H.; Li, Q.; Li, B.; Guo, Y.; Xing, J.; Xu, Q.; Liu, L.; Zhang, J.; Qi, W.; Jia, W.; et al. Continuous Reassortment of Clade 2.3.4.4 H5N6 Highly Pathogenetic Avian Influenza Viruses Demonstrating High Risk to Public Health. *Pathogens* **2020**, *9*, 670. [[CrossRef](#)]
- Lewis, N.S.; Banyard, A.C.; Whittard, E.; Karibayev, T.; Al Kafagi, T.; Chvala, I.; Byrne, A.; Meruyert Akberovna, S.; King, J.; Harder, T.; et al. Emergence and spread of novel H5N8, H5N5 and H5N1 clade 2.3.4.4 highly pathogenic avian influenza in 2020. *Emerg. Microbes Infect.* **2021**, *10*, 148–151. [[CrossRef](#)]
- Li, J.; Zhang, C.; Cao, J.; Yang, Y.; Dong, H.; Cui, Y.; Yao, X.; Zhou, H.; Lu, L.; Lycett, S.; et al. Re-emergence of H5N8 highly pathogenic avian influenza virus in wild birds, China. *Emerg. Microbes Infect.* **2021**, *10*, 1819–1823. [[CrossRef](#)] [[PubMed](#)]
- Gu, W.; Shi, J.; Cui, P.; Yan, C.; Zhang, Y.; Wang, C.; Zhang, Y.; Xing, X.; Zeng, X.; Liu, L.; et al. Novel H5N6 reassortants bearing the clade 2.3.4.4b HA gene of H5N8 virus have been detected in poultry and caused multiple human infections in China. *Emerg. Microbes Infect.* **2022**, *11*, 1174–1185. [[CrossRef](#)] [[PubMed](#)]
- Jiang, W.; Dong, C.; Liu, S.; Peng, C.; Yin, X.; Liang, S.; Zhang, L.; Li, J.; Yu, X.; Li, Y.; et al. Emerging Novel Reassortant Influenza A(H5N6) Viruses in Poultry and Humans, China, 2021. *Emerg. Infect. Dis.* **2022**, *28*, 1064–1066. [[CrossRef](#)] [[PubMed](#)]
- Hoffmann, E.; Stech, J.; Guan, Y.; Webster, R.G.; Perez, D.R. Universal primer set for the full-length amplification of all influenza A viruses. *Arch. Virol.* **2001**, *146*, 2275–2289. [[CrossRef](#)] [[PubMed](#)]
- Katoh, K.; Standley, D.M. MAFFT multiple sequence alignment software version 7: Improvements in performance and usability. *Mol. Biol. Evol.* **2013**, *30*, 772–780. [[CrossRef](#)]

16. Kalyaanamoorthy, S.; Minh, B.Q.; Wong, T.K.F.; von Haeseler, A.; Jermini, L.S. ModelFinder: Fast model selection for accurate phylogenetic estimates. *Nat. Methods* **2017**, *14*, 587–589. [[CrossRef](#)]
17. Nguyen, L.T.; Schmidt, H.A.; von Haeseler, A.; Minh, B.Q. IQ-TREE: A fast and effective stochastic algorithm for estimating maximum-likelihood phylogenies. *Mol. Biol. Evol.* **2015**, *32*, 268–274. [[CrossRef](#)]
18. Yang, L.; Zhu, W.; Li, X.; Bo, H.; Zhang, Y.; Zou, S.; Gao, R.; Dong, J.; Zhao, X.; Chen, W.; et al. Genesis and Dissemination of Highly Pathogenic H5N6 Avian Influenza Viruses. *J. Virol.* **2017**, *91*, e02199-16. [[CrossRef](#)]
19. Letunic, I.; Bork, P. Interactive Tree Of Life (iTOL) v5: An online tool for phylogenetic tree display and annotation. *Nucleic Acids. Res.* **2021**, *49*, W293–W296. [[CrossRef](#)]
20. Rambaut, A.; Lam, T.T.; Max Carvalho, L.; Pybus, O.G. Exploring the temporal structure of heterochronous sequences using TempEst (formerly Path-O-Gen). *Virus Evol.* **2016**, *2*, vew007. [[CrossRef](#)]
21. Baele, G.; Lemey, P.; Bedford, T.; Rambaut, A.; Suchard, M.A.; Alekseyenko, A.V. Improving the accuracy of demographic and molecular clock model comparison while accommodating phylogenetic uncertainty. *Mol. Biol. Evol.* **2012**, *29*, 2157–2167. [[CrossRef](#)] [[PubMed](#)]
22. Drummond, A.J.; Ho, S.Y.; Phillips, M.J.; Rambaut, A. Relaxed phylogenetics and dating with confidence. *PLoS. Biol.* **2006**, *4*, e88. [[CrossRef](#)] [[PubMed](#)]
23. Rambaut, A.; Drummond, A.J.; Xie, D.; Baele, G.; Suchard, M.A. Posterior Summarization in Bayesian Phylogenetics Using Tracer 1.7. *Syst. Biol.* **2018**, *67*, 901–904. [[CrossRef](#)] [[PubMed](#)]
24. Lemey, P.; Rambaut, A.; Drummond, A.J.; Suchard, M.A. Bayesian phylogeography finds its roots. *PLoS. Comput. Biol.* **2009**, *5*, e1000520. [[CrossRef](#)]
25. Huang, Y.; Niu, B.; Gao, Y.; Fu, L.; Li, W. CD-HIT Suite: A web server for clustering and comparing biological sequences. *Bioinformatics* **2010**, *26*, 680–682. [[CrossRef](#)]
26. Bielejec, F.; Baele, G.; Vrancken, B.; Suchard, M.A.; Rambaut, A.; Lemey, P. Spread3: Interactive Visualization of Spatiotemporal History and Trait Evolutionary Processes. *Mol. Biol. Evol.* **2016**, *33*, 2167–2169. [[CrossRef](#)]
27. Su, Y.; Yang, H.Y.; Zhang, B.J.; Jia, H.L.; Tien, P. Analysis of a point mutation in H5N1 avian influenza virus hemagglutinin in relation to virus entry into live mammalian cells. *Arch. Virol.* **2008**, *153*, 2253–2261. [[CrossRef](#)]
28. Yang, Z.Y.; Wei, C.J.; Kong, W.P.; Wu, L.; Xu, L.; Smith, D.F.; Nabel, G.J. Immunization by avian H5 influenza hemagglutinin mutants with altered receptor binding specificity. *Science* **2007**, *317*, 825–828. [[CrossRef](#)]
29. Imai, M.; Watanabe, T.; Hatta, M.; Das, S.C.; Ozawa, M.; Shinya, K.; Zhong, G.; Hanson, A.; Katsura, H.; Watanabe, S.; et al. Experimental adaptation of an influenza H5 HA confers respiratory droplet transmission to a reassortant H5 HA/H1N1 virus in ferrets. *Nature* **2012**, *486*, 420–428. [[CrossRef](#)]
30. Wang, W.; Lu, B.; Zhou, H.; Suguitan, A.L., Jr.; Cheng, X.; Subbarao, K.; Kemple, G.; Jin, H. Glycosylation at 158N of the hemagglutinin protein and receptor binding specificity synergistically affect the antigenicity and immunogenicity of a live attenuated H5N1 A/Vietnam/1203/2004 vaccine virus in ferrets. *J. Virol.* **2010**, *84*, 6570–6577. [[CrossRef](#)]
31. Bui, C.H.T.; Kuok, D.I.T.; Yeung, H.W.; Ng, K.C.; Chu, D.K.W.; Webby, R.J.; Nicholls, J.M.; Peiris, J.S.M.; Hui, K.P.Y.; Chan, M.C.W. Risk Assessment for Highly Pathogenic Avian Influenza A(H5N6/H5N8) Clade 2.3.4.4 Viruses. *Emerg. Infect. Dis.* **2021**, *27*, 2619–2627. [[CrossRef](#)] [[PubMed](#)]
32. Hiromoto, Y.; Yamazaki, Y.; Fukushima, T.; Saito, T.; Lindstrom, S.E.; Omoe, K.; Nerome, R.; Lim, W.; Sugita, S.; Nerome, K. Evolutionary characterization of the six internal genes of H5N1 human influenza A virus. *J. Gen. Virol.* **2000**, *81 Pt 5*, 1293–1303. [[CrossRef](#)] [[PubMed](#)]
33. Lycett, S.J.; Ward, M.J.; Lewis, F.I.; Poon, A.F.; Kosakovsky, S.L.; Brown, A.J. Detection of mammalian virulence determinants in highly pathogenic avian influenza H5N1 viruses: Multivariate analysis of published data. *J. Virol.* **2009**, *83*, 9901–9910. [[CrossRef](#)] [[PubMed](#)]
34. Spesock, A.; Malur, M.; Hossain, M.J.; Chen, L.M.; Njaa, B.L.; Davis, C.T.; Lipatov, A.S.; York, I.A.; Krug, R.M.; Donis, R.O. The virulence of 1997 H5N1 influenza viruses in the mouse model is increased by correcting a defect in their NS1 proteins. *J. Virol.* **2011**, *85*, 7048–7058. [[CrossRef](#)] [[PubMed](#)]
35. Zhang, J.; Li, X.; Wang, X.; Ye, H.; Li, B.; Chen, Y.; Chen, J.; Zhang, T.; Qiu, Z.; Li, H.; et al. Genomic evolution, transmission dynamics, and pathogenicity of avian influenza A (H5N8) viruses emerging in China, 2020. *Virus Evol.* **2021**, *7*, veab046. [[CrossRef](#)]
36. Karakus, U.; Thamamongood, T.; Ciminski, K.; Ran, W.; Gunther, S.C.; Pohl, M.O.; Eletto, D.; Jeney, C.; Hoffmann, D.; Reiche, S.; et al. MHC class II proteins mediate cross-species entry of bat influenza viruses. *Nature* **2019**, *567*, 109–112. [[CrossRef](#)]
37. Kwon, J.H.; Bahl, J.; Swayne, D.E.; Lee, Y.N.; Lee, Y.J.; Song, C.S.; Lee, D.H. Domestic ducks play a major role in the maintenance and spread of H5N8 highly pathogenic avian influenza viruses in South Korea. *Transbound Emerg. Dis.* **2020**, *67*, 844–851. [[CrossRef](#)] [[PubMed](#)]
38. Zhang, J.; Chen, Y.; Shan, N.; Wang, X.; Lin, S.; Ma, K.; Li, B.; Li, H.; Liao, M.; Qi, W. Genetic diversity, phylogeography, and evolutionary dynamics of highly pathogenic avian influenza A (H5N6) viruses. *Virus Evol.* **2020**, *6*, veaa079. [[CrossRef](#)]



39. Brown, J.D.; Stallknecht, D.E.; Swayne, D.E. Experimental infection of swans and geese with highly pathogenic avian influenza virus (H5N1) of Asian lineage. *Emerg. Infect. Dis.* **2008**, *14*, 136–142. [[CrossRef](#)]
40. Keawcharoen, J.; van Riel, D.; van Amerongen, G.; Bestebroer, T.; Beyer, W.E.; van Lavieren, R.; Osterhaus, A.D.; Fouchier, R.A.; Kuiken, T. Wild ducks as long-distance vectors of highly pathogenic avian influenza virus (H5N1). *Emerg. Infect. Dis.* **2008**, *14*, 600–607. [[CrossRef](#)]